 doi:10.20944/preprints202206.0339.v1

Article

New current oscillator for electrical bioimpedance spectroscopy

David W. C. Marcôndes [1], Pedro Bertemes-Filho[1,*] and A. S. Paterno [1]

[1] Universidade do Estado de Santa Catarina, Eng. Eletrica, Brasil; david.wcm@edu.udesc.br; pedro.bertemes@udesc.br;

* Correspondence: pedro.bertemes@udesc.br; +55 47 34817848

Version June 20, 2022 submitted to Journal Not Specified

Abstract: Current sources play an essential role in tissue excitation used in bioelectrical impedance spectroscopy. Most investigations use Howland current sources that, despite their practicality and simplified implementation, have operating frequency limitations and dependence on the load impedance due to theirs narrow output impedance, specially at higher frequencies. The objective of this work is to propose model for a robust current-controlled sinusoidal oscillator. The oscillator is based on fully analog electronics, which enables controlling oscillation phase and amplitude by using a voltage reference. The mathematical model is based on Pyragas control application to the classical harmonic oscillator. From the modelling process, it was build an oscillator topology based on second-generation current carriers and on transconductance amplifiers. The reference signal (F_{sync}) was a sinusoidal voltage source having a frequency of $1MHz$ and an amplitude of $1V_{pp}$. The oscillator output current synchronized the oscillations' phase and amplitude with F_{sync}, regardless of their magnitude before the control signal acted in the circuit at $t \approx 13.5\mu s$. SPICE simulations using ideal components have confirmed the successful operation of the proposed oscillator. This type of oscillator can be implemented in SOIC, then allowing oscillation control interface with logic circuits.

Keywords: Current Oscillator; Pyragas Model; Second-Generation Current Carrier; Bioimpedance Spectroscopy

1. Introduction

Approximately 800 million people worldwide do not have access to routine medical examinations [1]. Small urban centers often lack imaging equipment, such as CT scanners, as well as clinical analysis, specialized pediatric follow-up, among others, due to their high use and maintenance costs. Bioelectrical impedance spectroscopy (BIS) has proved to be a non-expensive and robust alternative to these tests in recent years, since it has been used in applications such as identifying small carcinomas [2], monitoring respiratory diseases in newborns [3], body composition analysis [4], among others. BIS enables performing non-invasive examinations, without exposing patients to harmful radiation or toxic agents, at relatively low construction costs. Recent advances achieved in BIS imaging systems have proved the effectiveness of this methodology in pre-clinical, diagnostic and follow-up examinations [5].

BIS often uses four electrodes placed on the investigated object (patient's tissue). A voltage-controlled current source (VCCS) is used to stimulate the aforementioned object within a pre-set frequency spectrum. This current, which circulates through a pair of external electrodes, generates a potential drop (response to the stimulus) in another pair of internal electrodes. Voltage is measured by an instrumentation system that enables finding the impedance spectrum. Both composition and extra and intracellular constituents of biological tissues are associated with the impedance spectrum [6]. Using a conductivity models enables one to find parameters capable of featuring electrical conductivity

 doi:10.20944/preprints202206.0339.v1

dispersion regions associated with cell wall, and it allows differentiating cells in a given tissue, as well as assessing tissue health.

Voltage-controlled current sources (VCCSs) used in BIS play fundamental role in the process to measure and feature different tissues. VCCSs, whose output impedance remains high (in the magnitude of M Ω) in at least three decades of frequency, play crucial role in limiting the resolution of images generated in electrical bioimpedance tomography systems [5]. The Howland current source, which is often used in this application type, presents output impedance with sensitive dependence on resistor (describe which resistor) matching, as well as open loop gain variation in operational amplifiers [7]. High-precision resistors arranged on the silicon wafer (on-chip resistors) increase the cost and limit the performance of the measurement system in integrated implementations (ASIC). However, the phase error in the vicinity of the dominant pole - associated with the output impedance - grows and affects the measurement of the imaginary component in the spectrum. It means that the operation happens at frequency range lower than the initially planned bandwidth.

On the other hand, the use of current-controlled oscillators in electrical bioimpedance spectroscopy has been poorly explored, so far [8]. Although sinusoidal and non-linear current oscillator circuits are well-known in the literature, adjustments in frequency, amplitude and oscillation conditions still fail to meet BIS's needs, when it does not use additional, complex and expensive electronic devices. Another issue lies on not knowing the phase of the generated signal, since it requires an additional system to enable synchronization with the data measurement and processing equipment. However, simple structures based on second-generation current carriers are a promising alternative to be used in BIS, since they are capable of reaching frequencies in the magnitude of a few tens of MHz and, consequently, of outperforming Howland current sources [9].

The aim of the current study is to propose a new current oscillator topology capable of meeting BIS's needs. This circuit combines the features of VCCS and sinusoidal oscillators. A reference sync signal input simultaneously provides phase, amplitude and oscillation condition control, by eliminating any additional electronic device used to control these parameters. The synchronization signal (in voltage) can be either sinusoidal or square wave, and it enables the interface with digital-logic circuits. The circuit used in synchronous operation mode follows both the phase and the amplitude of a given external reference signal. It is also possible operating in an autonomous (unsynchronized) manner, without control signal, since the circuit behaves like a sinusoidal oscillator in common current.

The herein proposed circuit is based on both current carriers and operational transconductance amplifiers (OTAs). All resistors and capacitors are earthed to enable their integrated implementation in a chip. Only two DC voltage signals are necessary for control and operation purposes: one for frequency control and one for synchronization. The output is formed by one current carrier and one OTA. This configuration enables two operating modes (i.e., with or without feedback), and it enables the excitation electrode's versatility to have, or not, direct reference to the grounding one. Unlike the solution proposed by [8], oscillator operation in the current study was absolutely analog, since it dismissed any internal digital-to-analog converters, analog filters and additional feedback structures. The oscillator can also be easily implemented on a bench, based on using easily-acquired components, in order to rule out the need of previous integration in wafer.

This work presents a mathematical description of the oscillator's operation by taking into account its dynamic model. The technique is proposed by Pyragas [10] to control and suppress chaos in nonlinear systems, which was adapted to the harmonic model by using simple harmonic oscillator equations. A circuit implementation is proposed, and then PSPICE simulations are conducted using ideal components for checking its functionality.

2. Mathematical framework

Simple harmonic oscillator dynamic equations can describe the behavior of all analog electronic sinusoidal oscillators. Thus, the behavior can be approached by the harmonic model, even in nonlinear systems, when producing pure sinusoidal oscillations [11]. Harmonic oscillations can be written in

Preprints (www.preprints.org) | NOT PEER-REVIEWED | Posted: 24 June 2022 doi:10.20944/preprints202206.0339.v1

two (equivalent) forms, namely: Eq. 1 and the set of Eqs. 2.The second form is mostly used for circuit analysis. Coefficients b and ω_0 determine oscillation condition and frequency, respectively. In practical terms, initial conditions x_0 and y_0 are defined by the initial charge applied on capacitors analogically. The solution could be obtained by integrating Eqs. 1 or 2.

$$\frac{d^2x}{dt^2} + b\frac{dx}{dt} + \omega_0^2 x = 0 \tag{1}$$

$$\begin{aligned} \frac{dx}{dt} &= -bx - \omega_0^2 y \\ \frac{dy}{dt} &= x \end{aligned} \tag{2}$$

The overall solution of Eq. 1 is:

$$y(t) = Asin(\omega_0 t + \phi) \tag{3}$$

where,

$$A = y_0^2 + \left(\frac{x_0}{\omega_0}\right)^2 \tag{4}$$

$$\phi = tan^{-1}\left(\frac{y_0\omega_0}{x_0}\right) \tag{5}$$

Equations 3, 4 and 5 shows that oscillation amplitude and phase are determined by initial conditions x_0 and y_0. Phase must be known based on reference to the initial time t_0, when the oscillator circuit starts its dynamics. However, determining the initial conditions of the circuit in an accurate manner means defining the initial charge applied on analog integration capacitors. In practice, it is very hard to be done if high accuracy is required. Thus, oscillator circuits use damping parameter b to trigger oscillations by momentarily placing the system in the divergence region of equation 1. Subsequently, the damping parameter is readjusted, after the required amplitude A is reached, to enable getting stable oscillations. According to the classic implementation of Wien bridge oscillator, a conforming amplifier, or an automatic gain control system, is used to guarantee oscillation stability by adjusting damping parameter b based on the oscillation amplitude.

Controlling oscillation phase and amplitude is of paramount importance for BIS. Although it is possible implementing a complex system to force the initial conditions, a simplified approach based on changes carried out in Eq. 2 was then here suggested. In order to do so, the linear forcing idealized by Pyragas, which is a method often used to control chaos in nonlinear systems, was included in Eqs. 2 [12]. The operating principle is quite simple, such as the F term in Eq. 6 continuously forces the oscillations until it reaches equality to an external reference signal, in the form of $A_2 sin(\omega_0 t + \phi')$. The F term vanishes when the system oscillates according to the external reference - the aforementioned equations are summarized in Eqs. 2, where $F \stackrel{\text{def}}{=} k(x_{ref} - x)$ is the Pyragas' factor, k is the forcing magnitude and x_{ref} is the external reference signal. Thus, this forcing process makes small corrections in oscillations whenever the dynamics diverges from the external reference.

$$\begin{aligned} \frac{dx}{dt} &= -bx - \omega_0^2 y \\ \frac{dy}{dt} &= x + F \end{aligned} \tag{6}$$

Preprints (www.preprints.org) | NOT PEER-REVIEWED | Posted: 24 June 2022 doi:10.20944/preprints202206.0339.v1

The parameter k plays critical role in controlling chaotic and non-linear systems. However, given the linearity of Eq. 1, the following simulations show flexibility in the selection of this parameter. Unfortunately, the arbitrariness of reference signal x_{ref}makes Eqs. 6 non-analytically integrable; thus, their solution must be based on numerical methods.

Figure 1 outlines the influence of parameter k on the numerical solution of Eqs. 6, wherein the fourth-order Runge Kutta finite element method was used. The graph shows variation in synchronization force F/x actuation rate, in comparison to dissipation parameter b and to forcing amplitude k. It is clear that the Pyragas' factor can guarantee oscillations in the system, even for $b \neq 0$, just by adjusting the k value in order to reduce control actuation.

The Pyragas' factor is approximately zero when oscillations reach a steady state; this factor makes the oscillation follow the external reference signal x_{ref}. In practical terms, parameter b is associated with the oscillation condition; therefore, it is possible concluding to conclude that the effective control actuation in the system does not require adjustments in the oscillation condition.

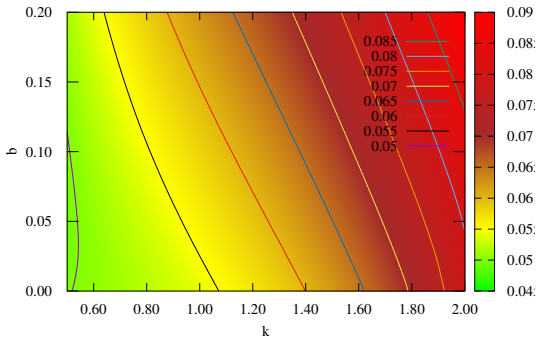

Figure 1. Pyragas' factor variation rate in comparison to damping factor b and to forcing amplitude k.

The external reference signal must have the same natural frequency of the system ω_0. during synchronized operations. When it happens, the oscillator's phase and amplitude are synchronized with the external reference signal. The Pyragas' factor, outside the resonance region between forcing and system, requires increasing the control actuation amplitude in order to stabilize the oscillations. Once the k value is fixed, forcing a reference signal outside the with a frequency different from ω_0 implies attenuating the amplitude, in comparison to x_{ref} as the difference increases, as shown in Figure 2. This phenomenon is particularly useful in BIS, since it enables using non-sinusoidal signals, such as square wave, as reference. In this case, the oscillator works as resonator filter, by extracting the fundamental frequency from the control signal and by attenuating the other harmonic components. This feature enables the interface with logic circuits.

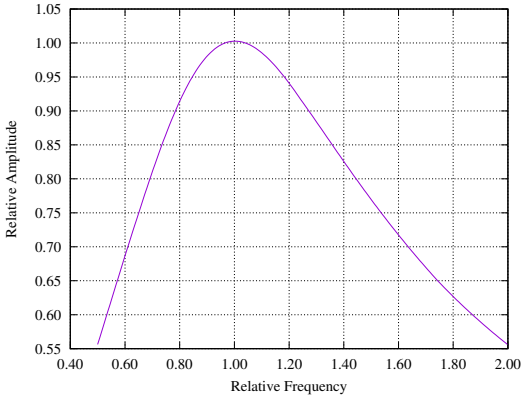

Figure 2. Rate of amplitude $max(x_{ext})/max(x)$ attenuation by relative frequency f_{ext}/f_o.

Preprints (www.preprints.org) | NOT PEER-REVIEWED | Posted: 24 June 2022 doi:10.20944/preprints202206.0339.v1

3. Electrical implementation of the oscillator

The oscillator described by Eqs. 6 is shown in Figure 3. Current carriers, along with capacitors C_1 and C_2 form analog integrators for variables x and y, respectively. The operational transconductance amplifier gm_2 accounts for the Pyragas' factor, and the synchronization signal is applied to its inverting input. On the other hand, gm_2 output must be disconnected from the circuit in desynchronized operations, where the circuit behaves like a common oscillator. Resistors R_1 and R_2 control the oscillation frequency and condition, respectively. The charge can be connected in two different ways: in a closed loop structure (feedback) or in an open loop structure (blue dotted line in Figure 3),The open loop structure dismisses one of the current carriers and enables direct reference to ground. Current output, which is seen as a VCCS whose input is F_{sync}, is scaled by transconductor gm_1.

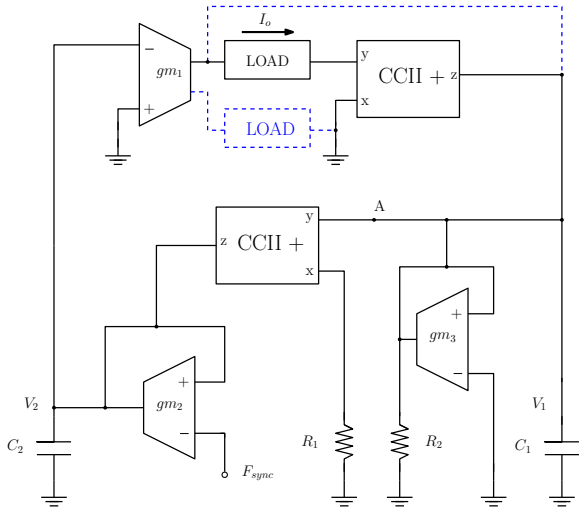

Figure 3. Proposed current oscillator. The current conveyors $CCII+$ are OPA860 and transconductors are LT1228

By naming the voltages on capacitors C_1 and C_2 as V_1 and V_2, the routine loop analysis shows that:

$$\frac{dV_1}{dt} = \frac{V_1}{C_1}\left(\frac{1}{R_2} - gm_3\right) - \frac{gm_1}{C_1}V_2$$

$$\frac{dV_2}{dt} = \frac{V_1}{C_2R_1} + \frac{gm_2}{C_2}(F_{sync} - V_2) \tag{7}$$

In order to compare these equations to Eqs. 6, it is necessary to dimensionlessize Eqs. 7. Therefore, one finds:

$$\overline{V}_1 = \frac{V_1}{C_1 R_1}$$

$$\overline{V}_2 = V_2 \left(\frac{gm_2}{C_2} \right)$$

$$\overline{F}_{sync} = F_{sync} \left(\frac{gm_2}{C_2} \right)$$

$$\tau = t \left(\frac{gm_2}{C_2} \right) \tag{8}$$

By replacing Eq. 8 in 7 and by comparing it to 6:

$$b = \left(\frac{1}{R_2} - gm_3 \right)$$

$$C_1 = C_2$$

$$\omega_0 = \sqrt{\frac{gm_1}{C_1^2 R_1}}$$

$$k = 1 \tag{9}$$

Pyragas' factor imposes $F_{sync} = V_2$ whenever the F_{sync} signal has the same frequency as ω_0 during synchronized operations. This voltage appears at the inverting input of transconductor gm_1. Therefore, the output current is:

$$I_o = -gm_1 F_{sync} \tag{10}$$

Equation 10 indicates that the circuit behaves like a VCCS, during synchronized operations. However, it is worth emphasizing that the output is sinusoidal regardless of whether F_{sync} s composed of different harmonic components, as indicated by the system's response to frequency mismatch (Figure 2). The natural oscillation frequency is adjusted by resistor R_1, which can be replaced by an additional element of transconductance, a digital potentiometer, or an analog multiplier placed at the high impedance input of the current carrier, and it enables controlling the frequency of oscillations with DC voltage signal. The Pyragas' factor dismisses the oscillation condition control, which makes it possible removing $gm3$ and R_2 from the circuit. However, whenever desynchronized operation is required, $gm3$ or R_2 can be adjusted so that factor b in Eq. 8 equals zero after oscillations reach a steady state.

It should be bear in mind that the output impedance of the oscillator does not only depend on transconductor $gm1$. Whenever the operation takes place in feedback mode, the charge current runs through the control loop and, then, it is adjusted by the Pyragas' factor. Based on Figure 2, when the operation takes place in resonance mode and disregards the non-idealities of transconductor $gm1$, the output current remains fixed to the external reference, since the control mediated by F_{sync} maintains oscillations' amplitude and phase. It means that, from the VCCS perspective, amplitude undergoes lesser attenuation as it gets closer to the resonance condition, and vice-versa. Therefore,

Preprints (www.preprints.org) | NOT PEER-REVIEWED | Posted: 24 June 2022 doi:10.20944/preprints202206.0339.v1

unlike the Howland current source, the output impedance has narrow peak over the natural oscillation frequency; it moves as this frequency changes. Secondary harmonics are quickly attenuated, and it means maximum impedance over the signal of interest; furthermore, it rules out the need of using additional impedance filters and converters to ensure current output stability.

Given the resonant feature of output impedance, it is worth investigating the oscillation frequency stability after the Pyragas' factor is introduced. Whenever the control destabilizes the oscillations, the resonance condition is not met and the output impedance decreases. Moreover, the Pyragas' factor does not change frequency stability at high and low frequency thresholds. Figure 3 shows the transfer function by breaking the loop at point A:

$$T(s) = \left(\frac{gm_1}{gm_3 + C_1 s}\right)\left(\frac{C_2 s + gm_2 - 1/R_3 + gm_2\mathcal{F}}{C_2 s + gm_2}\right) \tag{11}$$

Wherein $\mathcal{F} = F_{sync}/V_2$. Frequency stability is defined by [13]:

$$S_f = \left.\frac{d\phi(u)}{du}\right|_{u=1} \tag{12}$$

Wherein $u = s/j\omega_0$ and ϕ is the transfer function phase $T(s)$. The stability calculation process is based on an intricate algebraic equation that is not easily interpreted. However, it is possible to show that:

$$\frac{d}{d\mathcal{F}}\left(\lim_{\omega\to\infty} S_f\right) = 0 \tag{13}$$

In other words, stability at high frequencies is not affected by the Pyragas' factor. As for low frequencies, it is also possible to show that S_f does not depend on the Pyragas' factor, if:

$$C_2 gm_1 gm_3 + C_1 gm_1 gm_2 \ll \frac{gm_1 gm_3 gm_2 C_2}{1/R_1 + gm_2(1-\mathcal{F})} \tag{14}$$

Whenever the control acts in the oscillator, $\mathcal{F} = 1$ therefore, condition 14 is met as long as there is signal synchronization.

Figure 4 presents results of the transient simulation of the oscillator shown in Figure 3. Simulations took place in PSPICE environment and they took into account the ideal case of all components. The circuit was initially set to oscillate under pre-defined initial conditions in order to get different oscillation amplitudes and phases, as predicted through Eq. 4. The damping parameter was null, i.e., $gm_3 = 1/R_2$. The F_{sync} reference signal was connected to a sinusoidal voltage source at frequency of $1MHz$ and amplitude of $1V_{pp}$. The F_{sync} signal was multiplied by transconductance of $-1mA/V$ and this value was used as reference line (purple color) in the graph shown in Figure 4. Once the oscillations started, and after a $10\mu s$ transient was in place, a switch was used to connect the gm_2 output to the circuit at $t = 12\mu s$. After a transient of $\approx 1.5\mu s$, the oscillator output current synchronized the oscillations' phase and amplitude with F_{sync}, regardless of their magnitude before the control signal acted in the circuit at $t \approx 13.5\mu s$.

Figure 5 shows the phase synchronization process based on the external reference. The circuit was set to oscillate without actuating the forcing factor. Phase amplitude and difference (in comparison to the external reference signal) were determined by initial voltages at C_1 and C_2. The forcing factor was connected to the circuit at $t \approx 12\mu s$ in order to force the phase difference into zero. Phase synchronization process speed directly depends on forcing magnitude k and on initial phase difference in the oscillator.

Preprints (www.preprints.org) | NOT PEER-REVIEWED | Posted: 24 June 2022 doi:10.20944/preprints202206.0339.v1

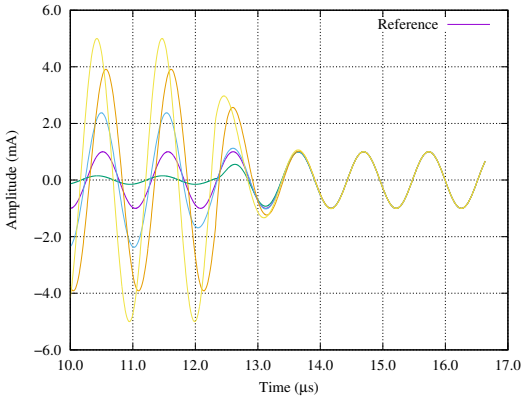

Figure 4. SPICE simulation of the oscillator (in ideal case) $gm_1 = gm_2 = gm_3 = 1/R_3 = 1mA/V$, $C_1 = C_2 = 10nF$, $R_1 = 1/(2\pi)^2 k\Omega$. F_{sync} is a sinusoidal voltage signal, with $1MHz$ and $1V_{pp}$.

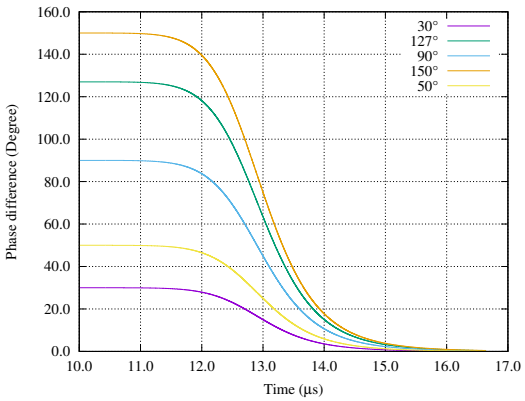

Figure 5. Oscillator phase synchronization. SPICE simulation of the oscillator in ideal phase. $gm_1 = gm_2 = gm_3 = 1/R_3 = 1mA/V$, $C_1 = C_2 = 10nF$, $R_1 = 1/(2\pi)^2 k\Omega$. F_{sync} is a sinusoidal voltage signal, with $1MHz$ and $1V_{pp}$.

The oscillator has two possible operating modes (Figure 6) depending on the output current and on its applications. A mirrored output transconductor, which corresponds to the blue dotted line in Figure 3, enables the direct connection of the charge to the ground and rules out the buffer formed by the current carrier. This approach reduces the likelihood of having common-mode voltage due to unbalance across the electrodes, without the need of adopting additional compensation loops. However, the output impedance becomes directly dependent on transconductor gm_1, since the rest of the circuit behaves like a voltage oscillator and produces a sinusoidal V_2. The direct connection to the ground also helps reducing electrodes' capacitance [6]. When the operation takes place in feedback mode, the output current is susceptible to corrections performed by the Pyragas' factor, and it increases output impedance under resonance condition. However, real current carriers present voltage offset in inputs x and y, and it can lead to common mode voltage errors, as well as to electrode capacitance increase due to electrolytic polarization. In the last case, and depending on the offset magnitude, it is necessary using decoupling capacitors at the output electrodes.

The initial condition control can be suppressed during the synchronized operation (right side of Figure 6), and it means removing R_2 and gm_3. The Pyragas' factor adjusts eventual deviations caused by components' non-idealities that imply $b \neq 0$. The desynchronized operation is featured by lack of synchronization signal and by the disconnection of the gm_2 output from the circuit. In this case, controlling the oscillation condition is of paramount importance, since small deviations implying $b > 0$ prevent oscillations from starting or from being quickly damped. Therefore, in this case, output current amplitude is not given by Eq. 10, but by the signal forming point over parameter $b \neq 0$, which is often seen in typical sinusoidal oscillator designs [14]. Although this operation type is possible, it is

Preprints (www.preprints.org) | NOT PEER-REVIEWED | Posted: 24 June 2022 doi:10.20944/preprints202206.0339.v1

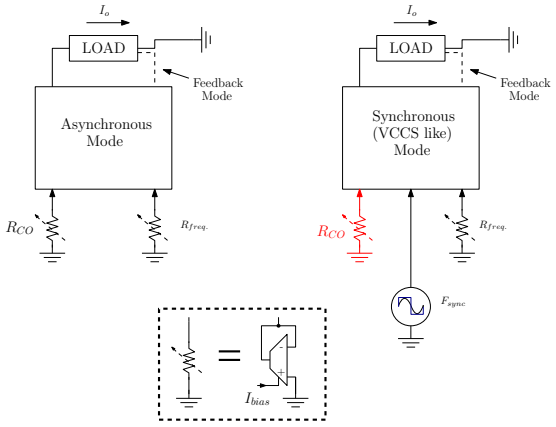

Figure 6. Oscillator operation types.

not interesting in BIS because it requires phase synchronization system, as well as additional control over oscillation amplitude and condition, and it takes away the advantages of including the Pyragas' factor in the system.

4. Conclusion

The proposed current oscillator presents features specifically aimed at BIS applications. Since it enables synchronizing both phase and amplitude with an external voltage signal, it does not require additional electronic devices to control and synchronize current output, a fact that solves the problem associated with using oscillators in BIS. According to numerical simulations, the source's output impedance is associated with natural oscillation frequency; this feature differs from that of VCCS, wherein oscillation frequency is often associated with the source's output poles. The oscillator presents maximum output impedance over the natural oscillation frequency, and it attenuates out-of-interest signals during sample excitation in the system. Attenuating unwanted signals in VCCS-based systems requires using additional filters and converters.

The proposed circuit has flexible application among different operating modes with and without feedback. It has simple electronics and its implementation might occupy a small area inside the silicon wafer. SPICE simulations focused on the ideal case have confirmed control actuation based on numerical simulations of dynamic equations. The Pyragas' factor does not change oscillation stability at high and low frequency thresholds; otherwise, it would imply reducing the output impedance of the whole circuit. The fact that all resistors and capacitors are directly connected to the ground wire makes it easy to implement this circuit in SOIC. The oscillation control interface with logic circuits can be mediated by a square wave signal that rules out the need of additional signal conditioning.

Conflicts of Interest: The authors declare no conflict of interest.

Abbreviations

The following abbreviations are used in this manuscript:

BIA	Bioimpedance analysis
ANN	Artificial neural networks
EMT	Effective Medium Theory

References

1. Group, W.B. Tracking universal health coverage : 2017 global monitoring report (English). *Washington, D.C. : World Bank Group* **2017**.
2. Sarode, G.S.; Sarode, S.C.; Kulkarni, M.; Karmarkar, S.; Patil, S. Role of bioimpedance in cancer detection: A brief review. *International Journal of Dental Science and Research* **2016**, *3*, 15 – 21.

3. Wu, Y.; Jiang, D.; Bardill, A.; de Gelidi, S.; Bayford, R.; Demosthenous, A. A High Frame Rate Wearable EIT System Using Active Electrode ASICs for Lung Respiration and Heart Rate Monitoring. *IEEE Transactions on Circuits and Systems I: Regular Papers* **2018**, *65*, 3810–3820. doi:10.1109/TCSI.2018.2858148.
4. González-Correa, C.H. Body Composition by Bioelectrical Impedance Analysis. In: Simini, F., Bertemes-Filho, P. (eds) Bioimpedance in Biomedical Applications and Research. *Springer, Cham* **2018**, *1*, 219–241. doi:10.1007/978-3-319-74388-2_11.
5. Lobo, B.; Hermosa, C.; Abella, A.; Gordo, F. Electrical impedance tomography. *Annals of translational medicine* **2018**, *6 2*, 26.
6. Sverre Grimnes, O.M. *Bioimpedance and bioelectricity basics*, 3 ed.; Vol. 4, Amsterdam : Academic Press, 2014.
7. Bertemes-Filho, P.; Felipe, A.; Vincence, V. High Accurate Howland Current Source: Output Constraints Analysis. *Circuits and Systems* **2013**, *4*, 451–458. doi:10.4236/cs.2013.47059.
8. Hong, S.; Jee, D. A 0.052 mm2, <0.4Bio-Impedance Measurement Using a Recursive Digital Oscillator and Current-Domain FIR Filter. *IEEE Transactions on Circuits and Systems II: Express Briefs* **2019**, *66*, 894–898. doi:10.1109/TCSII.2018.2870833.
9. Bertemes-Filho, P.; Vincence, V.C.; Santos, M.M.; Zanatta, I.X. Low power current sources for bioimpedance measurements: a comparison between Howland and OTA-based CMOS circuits. *Journal of Electrical Bioimpedance* **01 Jan. 2012**, *3*, 66 – 73. doi:https://doi.org/10.5617/jeb.380.
10. Pyragas, K. Continuous control of chaos by self-controlling feedback. *Physics Letters A* **1992**, *170*, 421 – 428. doi:https://doi.org/10.1016/0375-9601(92)90745-8.
11. Cook, P.A. *Nonlinear Dynamical Systems (2nd Ed.)*; Prentice Hall International (UK) Ltd.: GBR, 1994.
12. Fradkov, A.; Evans, R.; Andrievsky, B. Control of chaos: Methods and applications in mechanics. *Philosophical transactions. Series A, Mathematical, physical, and engineering sciences* **2006**, *364*, 2279–307. doi:10.1098/rsta.2006.1826.
13. Chang, C. Novel current-conveyor-based single-resistance-controlled/voltage-controlled oscillator employing grounded resistors and capacitors. *Electronics Letters* **1994**, *30*, 181–183. doi:10.1049/el:19940133.
14. Wiley, J. *Introduction to the Theory of Oscillations*; John Wiley and Sons, Ltd, 2015; chapter 1, pp. 1–10, [https://onlinelibrary.wiley.com/doi/pdf/10.1002/9783527695942.ch1]. doi:10.1002/9783527695author942.ch1.